Thermal stability of (0.15–0.35 wt%) rhodium on low-loaded ceria-supported rhodium catalysts

Franck Fajardie [a], Jean-François Tempere [b], Jean-Marie Manoli [b], Olivier Touret [c] and Gérald Djéga-Mariadassou [b,*]

[a] *Rhône-Poulenc, Centre de Recherches d'Aubervilliers, 52 rue de la Haie Coq, 93308 Aubervilliers Cedex, France*
[b] *Université P&M Curie, Laboratoire de Réactivité de Surface, CNRS UMR 7609, Case 178, T 54, 4 Place Jussieu, 75252 Paris Cedex 05, France*
E-mail: djega@ccr.jussieu.fr
[c] *Rhône Poulenc, Chimie Secteur I.O.M., Usine de La Rochelle, B.P. 2049, 17010 La Rochelle Cedex, France*

Received 27 April 1998; accepted 17 July 1998

The thermal stability of rhodium on ceric oxides submitted to high-temperature reduction (773–1173 K) and aging in air at 1173 K was studied by high-resolution transmission electron microscopy, X-ray photoelectron spectroscopy and benzene hydrogenation. Catalysts were prepared by anionic exchange of rhodium chloro complexes on both high (144 $m^2 g^{-1}$) and low specific surface area ceria (6 $m^2 g^{-1}$). In reducing conditions, both types of catalysts stabilized 5 nm metal rhodium particles. Calcination in air at 1173 K pointed out the interest of rhodium exchanged over a low surface precalcined ceria. In that case, all the metal remained at the surface of CeO_2 after calcination whereas 50% of the initial supported metal was buried into sintered ceria for the catalyst prepared from the high-surface CeO_2.

Keywords: rhodium catalysts, ceric oxide, HRTEM, XPS, particle size determination, thermal stability of rhodium particle after reduction and aging in air

1. Introduction

Numerous studies [1–3] have been recently devoted to the characterization and reactivity of CeO_2-supported rhodium systems active in the treatment of motor exhaust gases. The high activity and selectivity for NO reduction to N_2 makes rhodium one of the most interesting noble metals for three-way catalysts [4]. Elsewhere, due to its redox properties, ceria is essentially used for its capacity to store oxygen under oxidizing conditions for use under rich conditions [5–10].

As a matter of fact, Rh/CeO_2 systems are not favourable to HRTEM characterizations due to:

(a) the low contrast existing between metal rhodium and ceria;

(b) the reducible character of ceria which can lead, during reduction at high temperature, to partial or total encapsulation of metal particles by ceria [11,12];

(c) the possible burial of the metal phase into the bulk of the oxide support due to its sintering during treatments at high temperatures;

(d) the well known tendency of supported Rh to oxidize very easily even at room temperature [13,14].

This may be a reason why most of the electron microscopy studies concerning Rh/CeO_2 catalysts dealt with relatively high rhodium loadings (up to 4 wt% of the oxide support) supported over low surface area ceria supports. In view of the points mentioned above, it is clear that such conditions favour the observation of Rh^0 particles by this technique, however, they are not representative of commercial catalysts characteristics. In these studies, high percentages of metal rhodium exposed have been evidenced (metal particles of 1.2–2 nm in diameter), for 2.4 wt% Rh/(low-surface CeO_2) [15]. Some epitaxial relationship between metal and support has also been observed consisting in the growing of (111) planes of Rh^0 (lattice fringe spacing 0.22 nm) parallel to the same (111) planes of ceria (lattice fringe spacing 0.312 nm) [11,16]. Metal sintering or twinning as well as metal decoration or encapsulation by reduced ceria were rarely mentioned [11,12].

The present work reports on the stability of rhodium in Rh/CeO_2 catalysts containing low metal contents (0.15–0.35 wt% of the oxide support) *representative of commercial loadings.* Rhodium was introduced by anionic exchange on high and low surface area ceria supports. The latter case is of interest since it is recognized that the decrease in the specific surface area of the oxide support during high-temperature treatments, leads to a partial burial of the metal phase. Catalysts were also submitted to severe calcination and reduction treatments to simulate aging of real exhaust catalysts and were characterized by HRTEM, XPS and benzene hydrogenation. In line with a previous study [17], benzene hydrogenation was used, as a tool to evaluate the percentage of metal exposed of the reduced catalysts and to estimate average metal particle sizes when no direct evidence could be obtained by HRTEM analysis.

* To whom correspondence should be addressed.

2. Experimental procedure

2.1. Sample preparation

Ceria was a standard high specific surface area cerium oxide (144 $m^2\,g^{-1}$) provided by Rhône-Poulenc. It has been used for EOROII three-way catalysts (models of years 1993–1995). A low specific surface area ceria (6 $m^2\,g^{-1}$) was prepared by calcining in air the previous high surface area ceria. The calcination process (C) was as follows: ceria was heated to 673 K at a rate of 420 $K\,h^{-1}$ and was held at this temperature for 6 h. The temperature was then increased to 1173 K with the same rate and the sample held at this temperature for 6 h. Finally, the sample was cooled to ambient temperature in flowing air.

In all cases supported rhodium materials were prepared by the same anionic exchange process (E) with an acidic solution of $RhCl_3{\cdot}H_2O$ (Johnson and Matthey) adjusted with HCl at pH $\approx$ 2. The solids were filtered and dried in air for 3 h at 393 K. The amount of $RhCl_3{\cdot}3H_2O$ introduced into the solution was calculated to obtain metal loadings of 0.35 wt%. From these low loadings atomic rhodium dispersion was expected after anionic exchange [18].

Two samples were prepared and labelled as CeO_2(E) and CeO_2(CE). CeO_2(E) was prepared from the high specific surface area ceria (144 $m^2\,g^{-1}$) and contained 0.31 wt% Rh. CeO_2(CE) was prepared from the low surface area ceria (6 $m^2\,g^{-1}$) and contained 0.15 wt% Rh.

In order to study the thermal stability of the supported rhodium phase at high temperature and under oxidative atmosphere, sample CeO_2(EC) was also prepared by calcining CeO_2(E) in similar conditions to that previously described.

The reduced samples denoted (R) were treated for 2 h with hydrogen at various temperatures.

2.2. Characterization of the samples

The materials were characterized by the following methods.

BET surface measurements: Specific surface areas of samples were determined by physisorption of nitrogen at 77 K using a Quantasorb Jr. dynamic sorption system, linked to a thermal conductivity detector. The specific surface area was measured by the three-point BET method using nitrogen adsorption at different partial pressures.

HRTEM analysis: Samples studied by TEM were ground and dispersed in pure ethanol; the suspension was stirred in an ultrasonic bath and one drop was deposited on a carbon-coated grid. HRTEM images were performed with a JEOL JEM100 CXII apparatus equipped with a top entry device and operating at 100 kV.

XPS characterization: The XPS spectra of the various ceria supported rhodium samples were recorded on a spectrometer equipped with a non-monochromatized X-ray source (Mg K$\alpha_{1,2}$) and an electrostatic hemispherical analysis device working in a fixed analysis transmission (FAT) mode. Binding energies were corrected from charge effects by reference to the C 1s peak of carbon contamination, fixed at E(C 1s) = 285.0 eV. The pressure in the spectrometer chamber was approximately 5×10^{-9} Torr (760 Torr = 1 atm = 1.013×10^5 Pa) during data acquisitions. The reduced samples were transferred under vacuum from the reactor into sealed glass tubes and introduced into the spectrometer under argon atmosphere using a glove box. The experimental curve reconstruction was carried out using the commercial "Rainbow" software.

Benzene hydrogenation: Benzene hydrogenation measurements were carried out in a conventional system described elsewhere [17] and used as a method of determination of the percentage of rhodium exposed at the ceria surface. First of all, the number of metallic active sites (n_{exp}) can be easily calculated from the rate of benzene hydrogenation if the turnover rate of rhodium for the considered reaction is known at the temperature of the reaction. Then the ratio n_{exp}/n_{tot}, where n_{tot} is the total number of rhodium atoms present in the catalyst, leads to the percentage of metal exposed (D). From this latter calculation the particle size diameter (d, nm) was finally deduced as $d = 0.9/D$ [18]. It was assumed in all these calculations that the particles are spherical and that no rhodium atom was buried in the support after reduction or calcination.

3. Results and discussion

3.1. Stability of the Rh/CeO_2 catalysts under reducing atmosphere

Table 1 reports the main characteristics of supports and catalysts. It appears that almost all the rhodium content present in solution was exchanged (0.31 wt% instead of 0.35 wt%) on the high surface area ceria (CeO_2(E)), whereas only 50% was exchanged (0.15 wt% instead of 0.35 wt%) on the low surface area ceria (CeO_2(CE)). The relatively low yield obtained for sample CeO_2(CE) was attributed to the calcination treatment, which caused a drastic fall in the specific surface area of CeO_2 and a strong dehy-

Table 1
Specific surface areas and metal loadings of Rh/CeO_2 catalysts.

Sample[a]	Rh (%)	S ($m^2\,g^{-1}$)			
		Before reduction	After 2 h of reduction in pure H_2 at the given temperature		
			773 K	973 K	1173 K
CeO_2(E)	0.31	144	95	42	11
CeO_2(EC)	0.33	19	19	–	–
CeO_2(CE)	0.15	6	$\leqslant$6	$\leqslant$6	$\leqslant$6

[a] (E) for exchanged CeO_2 support; (EC) for CeO_2 support exchanged and calcined in air at 1173 K; (CE) for CeO_2 support precalcined in air at 1173 K and exchanged.

droxylation of its surface. Both phenomena were responsible for a significant decrease in the number of the surface OH_2^+ sites for anionic exchange.

3.1.1. HRTEM study of reduced CeO_2(E) and CeO_2(CE) samples

Table 2 reports HRTEM metal particle sizes observed for the CeO_2(ER) and CeO_2(CER) catalysts. As underlined in the introduction, the low rhodium loadings (<0.35 wt%) and the use of CeO_2 as support made difficult the HRTEM study. Moreover, small ceria crystallites could be easily mistaken for rhodium particles even for samples treated at 1173 K. Consequently, particles were identified as Rh^0 particles exclusively when lattice fringes spacing corresponding to Rh^0 could be measured.

No metal rhodium particles could be observed over reduced CeO_2(ER) samples obtained after reduction at temperatures lower than 1173 K (table 2). This was attributed to the poor contrast between Rh^0 particles and CeO_2 and to the substantial specific surface area retained by ceria after reduction (table 1) which limited the distinction between Rh^0 particles and remaining small ceria crystallites. However, after reduction at 1173 K, ceria presented large crystallites (about 30 nm in size) more or less dense which facilitated the detection of metal aggregates. In that case rhodium particles of 4–5 nm in diameter (figure 1) could be evidenced. Since particles which do not exceed 5 nm were observed after reduction at 1173 K, it was reasonably assumed that particles smaller or equal in size should exist for lower temperatures of reduction (table 2).

Table 2
Rhodium metal particle diameters measured by HRTEM over reduced CeO_2(ER) and CeO_2(CER) samples.

Catalyst	Rh (wt%)	Rh^0 particle diameter (nm) (after 2 h of reduction at the given temperature)[a]		
		773 K	973 K	1173 K
CeO_2(ER)	0.31	(⩽5.0)	(⩽5.0)	4.0–5.0
CeO_2(CER)	0.15	5.0	(⩽5.0)	5.0

[a] In parentheses: extrapolated size deduced from the diameters observed at higher temperatures of reduction.

Concerning reduced CeO_2(CER) samples, 5 nm metal particle sizes were observed for almost all the reduction temperatures (figure 2). Larger particles were not observed, even when reduction occurred at 1173 K which denoted a noticeable stability of the metal phase within the range of reduction temperatures investigated. Numerous cases of epitaxial growth of metal crystallite can be evidenced, it could be tempting to correlate this stability to the existence of metal–support interaction related to the epitaxial phenomena.

Metallic rhodium particles were more easily evidenced on reduced CeO_2(CER) samples because rhodium was supported on a precalcined low specific surface area ceria ($6\ m^2\,g^{-1}$). In these conditions the large planes of ceria favoured the detection of metal particles. Moreover, despite the lower amount of metal exchanged on calcined CeO_2 (0.15 wt%) compared to that exchanged on the high-surface CeO_2 (0.31 wt%), the surface rhodium precursor concentration was higher on CeO_2(CE) than on CeO_2(E) (respectively, $2.4\times10^{-6}\ mol\,m^{-2}$ and $2.1\times10^{-7}\ mol\,m^{-2}$). Consequently, after reduction at 773 K, the surface con-

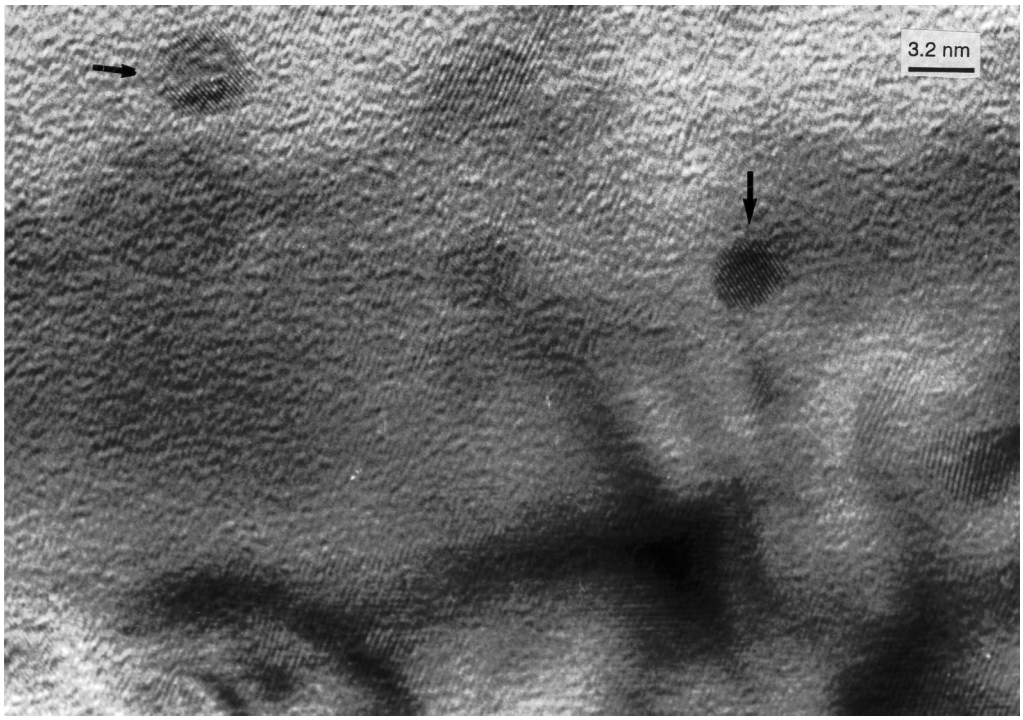

Figure 1. CeO_2(ER) samples reduced at 1173 K. HRTEM image for rhodium particles ((111) planes) denoted by arrows in planar projection on ceria.

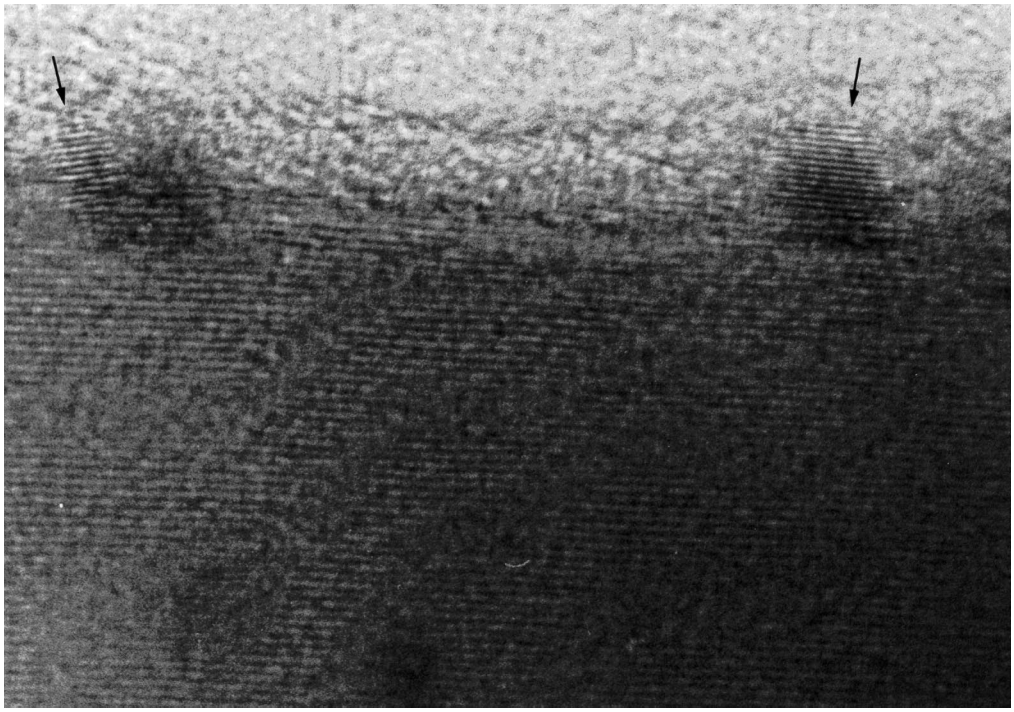

Figure 2. Rh/CeO_2(CER) reduced at 1173 K. HRTEM image in profile view. An epitaxial growth of one small rhodium particle ((111) plane) on ceria can be observed.

centration in Rh^0 particles was much larger for reduced CeO_2(CER) (230 particles of 5 nm per μm^2) than for reduced CeO_2(ER) (30 particles per μm^2 if particles of 5 nm are assumed). After reduction at 1173 K and due to the sintering of ceria, the surface concentration in Rh^0 particles of CeO_2(ER) strongly increased (350 particles of 5 nm per μm^2) while that of reduced CeO_2(CER) remained unchanged (230 particles of 5 nm per μm^2). This is consistent with the fact that Rh^0 particles could be observed on both samples reduced at 1173 K.

3.1.2. XPS study of samples as CeO_2(E) and CeO_2(CE) before and after reduction at 773 K

Complementary informations concerning the presence of rhodium at the ceria surface of samples non-reduced and reduced at 773 K were obtained by XPS. Here again the characterization of the Rh 3d signals was made difficult because of the very low rhodium loadings.

In the case of sample CeO_2(E) no rhodium signal was detected. Note that this sample had only been dried at 393 K after exchange and had not been reduced before analysis. At this time, exchanged rhodium complexes were expected to be dispersed on the surface of the oxide [19]. The absence of rhodium signal was related to the high specific surface area of the oxide support and to the high dispersion of supported rhodium ions obtained after the anionic exchange.

After reduction at 773 K of CeO_2(E) two peaks were observed, respectively located at 307.4 and 312.4 eV (figure 3(a)). They were ascribed to the $3d_{(3/2-5/2)}$ levels of rhodium metal with a characteristic 5 eV spin–orbit coupling. The position of the maxima of the peaks suggests that Rh^0 would be found on this sample, however, the broadness of the lines could indicate the presence of rhodium in other oxidation states (for example, Rh^+ whose maxima are located at 312.9 for Rh $3d_{3/2}$ and 308.1 eV for Rh $3d_{5/2}$). The low intensity of Rh 3d signals could obviously be related to the low surface concentration in rhodium due to the relatively high surface area retained by CeO_2 after reduction at 773 K (95 $m^2\,g^{-1}$, table 1).

In the case of CeO_2(CE) and in spite of a poor rhodium signal to background ratio, two peaks located at 310.5 and 315.5 eV could be reasonably ascribed to the $3d_{(3/2-5/2)}$ (figure 3(b)) levels of Rh^{3+} [13]. The XP signals of Rh^{3+} could be detected for CeO_2(CE) due to its higher surface concentration in rhodium ions compared to that present over the CeO_2(E) sample.

Intense and particularly well resolved Rh^0 signals were evidenced on the CeO_2(CER) sample after reduction at 773 K (figure 3(c)). The remarkable intensities of the XP Rh^0 signals, compared to those observed for reduced CeO_2(ER), were again related to a higher surface concentration of particles (230 particles per μm^2 of the oxide support). Two peaks were located at 307.5 and 312.5 eV, and attributed to the Rh^0 $3d_{(5/2-3/2)}$ levels. The asymmetric shape appearing on the high binding energy side of the Rh 3d peak (figure 3(c)) was ascribed to the Doniach–Sunjic effect [20], which is characteristic of metals such as Pt^0, Pd^0 and Rh^0 with high density of states at the Fermi level [21]. The relatively small values of the Rh^0 line widths, and the occurrence of the Doniach–Sunjic effect, confirm HRTEM observations according to which rhodium was totally reduced as 5 nm metal aggregates after reduction at 773 K.

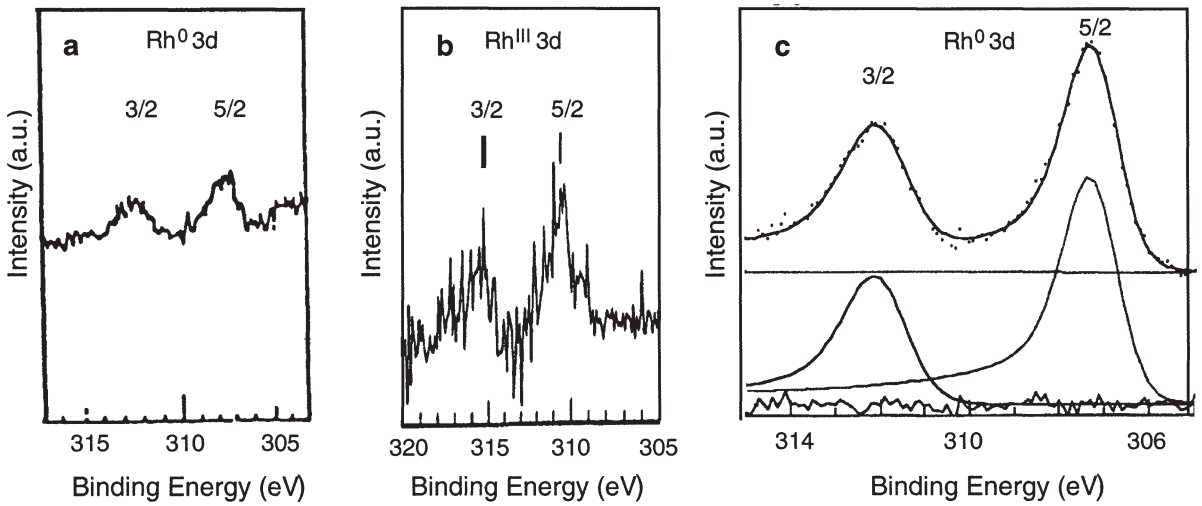

Figure 3. (a) XP spectrum of Rh^0 3d for CeO_2(ER) reduced at 773 K; (b) XP spectrum of Rh^{III} 3d for unreduced CeO_2(CE); (c) XP spectra of Rh^0 3d for CeO_2(CER) reduced at 773 K: experimental data (upper) and reconstruction (lower) of the Rh 3d signals using the theoretical Doniach–Sunjic formula [20].

It clearly appeared from these results that both XPS and HRTEM analysis are limited by the low metal loading and the subsequent specific surface area retained by the oxide support. In order to complete HRTEM and XPS data, benzene hydrogenation was performed on these samples.

3.2. Stability of the rhodium metal phase under reducing atmosphere

Considering the difficulties accounted for HRTEM to identify the metal phase over Rh/CeO_2 samples, it remained to precise whether particle sizes observed by electron microscopy were representative of a mean size.

In this section it will be shown that benzene hydrogenation could be used to determine average metal rhodium particle sizes. This was of particular interest since metal particles were not systematically observed by electron microscopy. Recall metal rhodium particles were assumed spherical and it was considered that the totality of the metal was at the surface of ceria. This latter assumption was justified for all samples derived from CeO_2(CE) and for sample CeO_2(ER) reduced at 773 K since, after reduction of these catalysts, only small changes in specific surface area of ceria were observed (table 1).

Secondly, it will be shown that the percentages of metal exposed obtained from benzene hydrogenation could also be used, in relation with HRTEM observations, to provide information concerning the occurrence of metal decoration and encapsulation by reduced ceria.

3.2.1. Benzene hydrogenation as a tool to determine metal particle sizes. Case of samples reduced at 773 K

Table 3 lists the percentages of metal exposed obtained for CeO_2(E) and CeO_2(CE) reduced at 773 K. In the case of sample CeO_2(CER) reduced at 773 K, 5 nm metal rhodium particles were observed by HRTEM and benzene hydrogenation predicted 4.5 nm (table 3). For CeO_2(ER) reduced at 773 K, benzene hydrogenation assumed particle sizes of 4 nm (table 3). HRTEM showed no metal particles for this temperature of reduction but it was shown earlier in this study that particle sizes less or equal to 5 nm were expected.

Table 3
Percentages of metal exposed and rhodium particle sizes of Rh/CeO_2 catalysts reduced at 773 K.

Sample	Percentage of exposed Rh^0 [a]	d (nm) by benzene hydrog.[b]	d (nm) by HRTEM[c]
CeO_2(ER)	20.0	4.0	($\leqslant$5.0)
CeO_2(ECR)	5.3	14.0 [7.5]	$\leqslant$7.5
CeO_2(CER)	18.6	4.5	5.0

[a] Percentages of metal exposed determined by benzene hydrogenation.
[b] Average diameters of metal rhodium particles deduced from the percentages of metal exposed as measured by benzene hydrogenation. In brackets: average size calculated when considering that 46.5% of the metal was buried into sintered CeO_2 after calcination.
[c] Diameters of metal rhodium particles observed by HRTEM. In parentheses: extrapolated size deduced from the diameters observed at higher temperatures of reduction.

Due to the fairly good agreement existing between particle sizes determined from benzene hydrogenation and those obtained by HRTEM for both reduced samples, the particle sizes estimated by benzene hydrogenation for samples reduced at 773 K were taken as the average particle diameters. This implied, in agreement with the first predictions, that after reduction at 773 K, the total metal loading remained at the surface of both catalysts as 4–5 nm metal rhodium particles, free of any decoration or encapsulation phenomena.

At this point of the study, it is interesting to note that, in reducing conditions, the metal phase was as stable over the high and the low specific surface area ceria, since both catalysts exhibited Rh^0 particles of about 5 nm in diameter even after reduction at 1173 K.

It can be seen from the previous findings that benzene hydrogenation can be used to estimate metal particle sizes.

However, as discussed in the following section, this technique is restricted to catalysts for which the totality of the metal loading was at the surface of the oxide support and without any interaction with it (no decoration nor encapsulation phenomena). In the case of the CeO_2(ECR) sample, 7.5 nm rhodium particles were observed by TEM after reduction at 773 K. This value strongly differs from that obtained using the benzene hydrogenation method. Such a disagreement could be related to the burial of part of the rhodium content into the bulk of the sintered CeO_2 or to the migration of rhodium ions into the ceria lattice during the calcination step [22]. Assuming that the rhodium particle size is effectively 7.5 nm, one can deduce that about 50% (46.5%) of the rhodium phase has been buried.

3.2.2. Stability of rhodium upon temperature of reduction, evidence of the occurrence of metal coverage and burial at high temperature of reduction

In order to test the stability of the metal phase in reducing conditions, CeO_2(E) and CeO_2(CE) were reduced in pure hydrogen at increasing temperatures.

The stability of the metal phase (table 4) on the reduced CeO_2(ER) and CeO_2(CER) samples was investigated by comparison of the percentages of metal exposed determined by benzene hydrogenation with the particle sizes which could be obtained by microscopy. The evolution of the percentages of metal exposed versus temperature of reduction are presented in table 4. For both samples the percentages of metal exposed decreased with increasing temperature of reduction which seemed to indicate that sintering of the metal phase occurred. However, HRTEM showed that rhodium was still present as 5 nm metal particles even after reduction at 1173 K which, by contrast, indicated a good stability of the metal phase. This apparent contradiction could be explained in term of decoration and encapsulation of Rh^0 aggregates by reduced ceria. Actually, the decrease of the percentages of metal exposed with the increase of the temperature of reduction could suggest that decoration of the metal particles by reduced ceria occurred progressively for temperatures of reduction higher than 773 K. Catalysts obtained after reduction at 1173 K no more display hydrogenating properties. Considering the evidence of Rh^0 in the XP spectrum of the catalysts reduced at 773 K, rhodium metal was expected after reduction at 1173 K. Consequently, the loss of hydrogenating character of these samples suggested that the totality of the metal was encapsulated by the reduced support. The occurrence of decoration by ceria would explain why the catalysts reduced at 1173 K exhibited 5 nm metal particles and were, however, quasi inactive in benzene hydrogenation.

Table 4
Percentages of metal exposed versus temperature of reduction for CeO_2(E) and CeO_2(CE).

	Rh (wt%)	Percentage of metal exposed after direct reduction and after oxidation/reduction cycle				
		773 K[a]	973 K[a]	Ox/Red[b]	1173 K[a]	Ox/Red[b]
CeO_2(ER)	0.31	20.0	9.3	23.1	$\leqslant$1.0	7.1
CeO_2(CER)	0.15	18.6	13.5	32.2	$\leqslant$1.0	5.5

[a] Direct reduction at the column indicated temperature.
[b] Direct reduction at the indicated temperature followed by oxidation for 2 h at 673 K in a 5 vol% O_2/Ar mixture (5 $l\,h^{-1}$) finally followed by 2 h of reduction at 573 K.

HRTEM analysis of these samples namely evidenced several 5 nm aggregates which were identified as Rh^0 particles. Note as well that other 5 nm aggregates were observed but could not be identified as Rh^0 particles since their lattice fringe spacings could not be resolved. These aggregates, in agreement with the inactivity observed for benzene hydrogenation, were tentatively ascribed to metal particles covered with reduced ceria. Moreover, it cannot be excluded that the particles for which Rh^0 lattice fringe spacings could be measured were also covered by a fine ceria layer.

To confirm the occurrence of some encapsulation for high reduction temperature, reduced samples were oxidized at 673 K in a O_2(5 vol%)/Ar gas mixture and reduced at lower temperature (573 K). The resulting percentages of metal exposed are presented in table 4. For all samples more metal was exposed after oxidation and subsequent reduction, even for those which exposed no metal after direct reduction at 1173 K. These results confirmed that metal particles were partly or completely covered with reduced CeO_2 after direct reduction carried out above 773 K. Moreover, the fact that the percentages of metal exposed, obtained after the oxidation–reduction treatment, were higher than that corresponding to the HRTEM particle sizes measured before oxidation may indicate a redispersion of the metal during the oxidation treatment.

For samples reduced at 773 K, as discussed earlier, the agreement existing between metal particle sizes determined by benzene hydrogenation and those obtained by HRTEM, indicates that all the rhodium was located at the surface of CeO_2 and that no decoration occurred. Consequently, the relatively low percentages of metal exposed measured after direct reduction at 773 K were attributed to metal sintering.

4. Conclusions

Thermal stability of rhodium in low-loaded rhodium ceric oxides (0.15–0.35 wt%) was studied in reducing atmosphere and after oxidation–reduction cycles. As HRTEM and XPS techniques were limited by the low metal loadings of catalysts and the relatively high surface areas of the oxide supports, benzene hydrogenation was used to determine the percentage of metal exposed of these catalysts. As long as rhodium remained fully accessible at the external surface of ceria, the percentages of metal exposed could be used to determine metal particle sizes in good agreement with those obtained by HRTEM (when available).

In revenge when some loss of metal accessibility occurs by metal coverage by ceria and/or burial the benzene hydrogenation method leads to false value. But the percentages of metal exposed could be used in relation with HRTEM data to evidence the loss of metal accessibility during the high-temperature treatments.

So, HRTEM measurements showed that rhodium particle sizes were found to be as stable on a calcined low surface area ceria as a function of the reduction temperature (from 773 to 1173 K).

Concomitantly it was observed that the percentage of metal exposed strongly decreased with the reduction temperature which could strongly suggest some increasing coverage or burial of the metal by the support, since no metal sintering could be evidenced by HRTEM. Furthermore, the surface regeneration capability after oxidation–reduction cycles could be in agreement with the occurrence of reversible encapsulation phenomena, and irreversible burial contribution.

In line with catalysts used for post-combustion applications, this study showed that it might be interesting to deposite the metal over calcined oxide supports. Actually, it was shown that rhodium was as stable over calcined ceria as over a high-surface ceria. Such systems would also permit to limit the burial of the metal into the bulk of the oxide support during high-temperature calcinations and thus should contribute to a decrease of the initial amount of metal to be introduced on the post-combustion catalysts supports.

Acknowledgement

The authors greatly acknowledge CNRS and Rhône-Poulenc for their financial grant. The technical assistance of M. Lavergne in the HRTEM measurements and of H. Roulet and G. Dufour in the XPS study are also gratefully acknowledged. JMM and JFT want to thank C. Potvin for helpful discussions.

References

[1] B. Harrisson, A.F. Diwells and C. Hallet, Plat. Met. Rev. 32 (1988) 73.
[2] S. Bernal, F.J. Botana, J.J. Calvino, G.A. Cifredo, J.A. Pérez-Omil and J.M. Pintado, Catal. Today 23 (1995) 219.
[3] G. Leclercq, C. Dathy, G. Mabilon and L. Leclercq, *Catalysis and Automotive Pollution Control II*, ed. A. Crucq (Elsevier, Amsterdam, 1991) p. 181.
[4] M. Shelef and G.W. Graham, Catal. Rev. 36 (1994) 433.
[5] S. Kacimi, J. Barbier, Jr., R. Taha and D. Duprez, Catal. Lett. 22 (1993) 343.
[6] J.C. Summers and S.A. Ausen, J. Catal. 58 (1979) 131.
[7] G. Kim, Ind. Eng. Chem. Prod. Res. Dev. 21 (1982) 267.
[8] K.C. Taylor, in: *Catalysis Science and Technology*, Vol. 5, eds. J.R. Anderson and M. Boudart (Springer, Berlin, 1984).
[9] H.C. Yao and Y.F. Yu-Yao, J. Catal. 86 (1984) 254.
[10] P. Fornasiero, R. Di Monte, G. Ranga Rao, J. Kaspar, S. Meriani, A. Trovarelli and M. Graziani, J. Catal. 151 (1995) 168.
[11] S. Bernal, G. Blanco, J.J. Calvino, J.A. Pérez-Omil, J.M. Pintado and A. Varo, in: *New Developments in Selective Oxidation II*, eds. V. Cortés Corberan and S. Vic Bellon (Elsevier, Amsterdam, 1994) p. 507.
[12] M. Pan, J.M. Cowley and R. Garcia, Micron Microsc. Acta 18 (1987) 165.
[13] G. Munera, A. Fernandez and A.R. Gonzalez-Elipe, in: *Catalysis and Automotive Pollution Control II*, ed. A. Crucq (Elsevier, Amsterdam, 1991) p. 207.
[14] J.P. Holgado and G. Munera, in: *3rd International Congress on Catalysis and Automotive Pollution Control*, Vol. 2, eds. A. Frennet and J.M. Bastin (Elsevier, Amsterdam, 1994).
[15] S. Bernal, J.J. Calvino, M.A. Cauqui, G.A. Cifredo, A. Jobacho and J.M. Rodriguez-Izquierdo, Appl. Catal. A 99 (1993) 1.
[16] S. Bernal, F.J. Botana, J.J. Calvino, M.A. Cauqui, G.A. Cifredo, A. Jobacho, J.M. Pintado and J.M. Rodriguez-Izquierdo, J. Phys. Chem. (1993) 4118.
[17] F. Fajardie, J.F. Tempere and G. Djéga-Mariadassou, J. Catal. 163 (1996) 77.
[18] M. Boudart and G. Djéga-Mariadassou, *Kinetics of Heterogeneous Catalytic Reactions* (Princeton University Press, Princeton, 1984).
[19] Y.-F. Yu-Yao and J.T. Kummer, J. Catal. 106 (1987) 307.
[20] S. Doniach and M. Sunjic, J. Phys. Chem. 3 (1970) 285.
[21] S. Hufner and G.K. Wertheim, Phys. Rev. B 11 (1971) 678.
[22] S. Imamura, T. Yamashita, R. Hamada, Y. Saito, Y. Nakao, N. Tsuda and C. Kaito, J. Mol. Catal. A 129 (1998) 249.